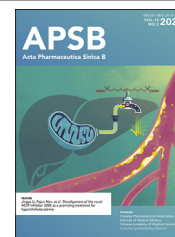




Chinese Pharmaceutical Association  
Institute of Materia Medica, Chinese Academy of Medical Sciences

Acta Pharmaceutica Sinica B

[www.elsevier.com/locate/apsb](http://www.elsevier.com/locate/apsb)  
[www.sciencedirect.com](http://www.sciencedirect.com)



ORIGINAL ARTICLE

# PAFR/Stat3 axis maintains the symbiotic ecosystem between tumor and stroma to facilitate tumor malignancy



Di Zhao<sup>a,b,†</sup>, Jing Zhang<sup>a,†</sup>, Lingyuan Zhang<sup>a</sup>, Qingnan Wu<sup>a,b,c</sup>,  
Yan Wang<sup>a,b,c</sup>, Weimin Zhang<sup>a,b,d</sup>, Yuanfan Xiao<sup>a</sup>, Jie Chen<sup>a,b,c,\*</sup>,  
Qimin Zhan<sup>a,b,c,d,\*</sup>

<sup>a</sup>Key Laboratory of Carcinogenesis and Translational Research (Ministry of Education/Beijing), Laboratory of Molecular Oncology, Peking University Cancer Hospital & Institute, Beijing 100142, China

<sup>b</sup>Research Unit of Molecular Cancer Research, Chinese Academy of Medical Sciences, Beijing 100021, China

<sup>c</sup>Peking University International Cancer Institute, Beijing 100191, China

<sup>d</sup>Shenzhen Bay Laboratory, Shenzhen 518132, China

Received 29 January 2022; received in revised form 17 June 2022; accepted 7 August 2022

## KEY WORDS

Esophageal squamous cell carcinoma;  
Cancer-associated fibroblasts;  
PAFR;  
Stat3;  
G-protein-coupled receptor;  
JAK2;  
IL-6;  
IL-11

**Abstract** Stroma surrounding the tumor cells plays crucial roles for tumor progression. However, little is known about the factors that maintain the symbiosis between stroma and tumor cells. In this study, we found that the transcriptional regulator-signal transducer and activator of transcription 3 (Stat3) was frequently activated in cancer-associated fibroblasts (CAFs), which was a potent facilitator of tumor malignancy, and formed forward feedback loop with platelet-activating factor receptor (PAFR) both in CAFs and tumor cells. Importantly, PAFR/Stat3 axis connected intercellular signaling crosstalk between CAFs and cancer cells and drove mutual transcriptional programming of these two types of cells. Two central Stat3-related cytokine signaling molecules-interleukin 6 (IL-6) and IL-11 played the critical role in the process of PAFR/Stat3 axis-mediated communication between tumor and CAFs. Pharmacological inhibition of PAFR and Stat3 activities effectively reduced tumor progression using CAFs/tumor co-culture xenograft model. Our study reveals that PAFR/Stat3 axis enhances the interaction between tumor and its associated stroma and suggests that targeting this axis can be an effective therapeutic strategy against tumor malignancy.

\*Corresponding authors.

E-mail addresses: [zhanqimin@bjmu.edu.cn](mailto:zhanqimin@bjmu.edu.cn) (Qimin Zhan), [cj\\_blue@126.com](mailto:cj_blue@126.com) (Jie Chen).

<sup>†</sup>These authors made equal contributions to this work.

<https://doi.org/10.1016/j.apsb.2022.08.014>

2211-3835 © 2023 Chinese Pharmaceutical Association and Institute of Materia Medica, Chinese Academy of Medical Sciences. Production and hosting by Elsevier B.V. This is an open access article under the CC BY-NC-ND license (<http://creativecommons.org/licenses/by-nc-nd/4.0/>).

## 1. Introduction

Cancer-associated fibroblasts (CAFs), the activated fibroblasts, constitute the major stromal components in many types of malignancies, especially epithelial-derived cancers<sup>1,2</sup>. Accumulating evidences suggest that CAFs are the master regulator of many diverse stromal programs and cancer cell signaling pathways through producing various cytokines, chemokines to create a permissive track for tumor malignancy<sup>3,4</sup>. Especially, CAFs can promote malignant progression of tumor *via* inducing proliferation, migration, lymph node metastasis, or chemoresistance of tumor cells<sup>5–8</sup>. Some stromal expression molecules, including hydrogen peroxid-inducible clone 5 (HIC-5)<sup>9</sup>, Twist1<sup>10</sup>, or nuclear factor- $\kappa$ B (NF- $\kappa$ B)<sup>11</sup>, can facilitate the tumor-promoting function of CAFs and serve as diagnostic markers for solid tumors. However, the precise cellular and molecular mechanisms that connect intercellular communications between stroma and cancer cells and resultantly reinforce mutual reprogramming of these two types of cells are still largely unknown.

Among various tumor-promoting transcriptional factors, signal transducer and activator of transcription 3 (Stat3) is ubiquitously expressed and activated by various stresses, such as cytokines, chemokines, and several growth factors<sup>12–14</sup>. Intratumoral Stat3 activation has been shown to play a fundamental role in tumor initiation and progression. Depletion of Stat3 markedly reduces growth, metastasis, angiogenesis, and other important tumor related phenotypes<sup>15–17</sup>. In clinical analyses, activation of Stat3 is strongly related to disease progression in mammary, colorectal, lung cancer, and so on<sup>16,18,19</sup>. Stat3 is also activated in the cellular components of tumor microenvironment. Stromal Stat3 promotes tumour cell survival and angiogenesis *via* modulating various cytokines production [for example, interleukin 6 (IL-6), epidermal growth factor (EGF), transforming growth factor  $\beta$  (TGF- $\beta$ ) and vascular endothelial growth factor (VEGF)]<sup>20,21</sup>. Mechanistically, Stat3 is recruited, phosphorylated by Janus kinases (JAKs) to translocate into the nucleus and promotes the transcription of various essential tumor-promoting genes expression<sup>22</sup>. The activation of Stat3 is under the stimulation of the signaling from proinflammatory cytokines, especially IL-6 and its family members, such as IL-11, and multiple coordinated signaling proteins, including G protein-coupled receptors (GPCRs), Toll-like receptors (TLRs). Stat3 and its related cytokines or signaling proteins form a tightly regulated feed-forward feedback loop that takes Stat3 as the core to induce the malignancy of tumor cells.

It is curious that whether activated stromal Stat3 plays a complementary, and perhaps equally important role, in educating the stroma to a protumorigenic state. Platelet-activating factor receptor (PAFR), a G-protein-coupled receptor (GPCR) hyperactivated in ESCC cells, has been reported to tightly correlate with the activation of intratumoral signaling pathways and esophageal squamous cell carcinoma (ESCC) malignancy<sup>23</sup>. However, the possible molecular mechanisms of Stat3/PAFR axis-mediated signaling crosstalk between cancer and stromal cells, as well as its potential therapeutic implications are needed further explored.

## 2. Methods

### 2.1. Antibodies and reagents

The exact information of antibodies and reagents was listed in Supporting Information [Table S1](#).

### 2.2. Cell lines and transfection

The human ESCC cell lines-KYSE410, KYSE150 (generously provided by Dr. Shemada of Kyoto University, Japan) were cultured in complete Roswell Park Memorial Institute (RPMI) 1640 medium. Human primary ESCC cells and their paired CAFs were purchased from CHI Scientific, Inc. (Jiangyin, China). All cells were confirmed to be mycoplasma-free and maintained at 37 °C in a humidified 5% CO<sub>2</sub> incubator.

For knockdown experiments, short hairpin (sh) ribonucleic acid (RNA) targeting human PAFR and Stat3 were used. The exact information of shRNA sequence was shown in Supporting Information [Table S2](#). shRNAs were transfected using Lipofectamine 2000 into ESCC cells with 60% confluence following the manufacturer's protocol. Transfection mix solution was replaced by RPMI 1640 containing 1  $\mu$ g/mL puromycin for selection after 48 h. Stable cell line pcDNA3.1-Flag-PAFR D289A plasmid was stably transfected into indicated ESCC cells, and transfection efficacy was evaluated using immunoblotting.

### 2.3. Chromatin immunoprecipitation (ChIP)-on-chip

Primary ESCC cells and paired CAFs were crosslinked using 1% formaldehyde for 10 min. Cells were put into lysis buffer after washed with cold phosphate-buffered saline solution (PBS). Nuclear extracts were collected and chromatin fragments were obtained using ultrasonicator. Then, sonicated chromatin was resuspended in immunoprecipitation (IP) buffer and incubated with 10  $\mu$ g ChIP grade pStat3 Tyr<sup>705</sup> antibody overnight at 4 °C. 30  $\mu$ L of protein A/G beads were incubated with this IP for 4 h. After washed four times, the DNA was then recovered by reversing the crosslinks, and purified by Qiagen purification kit. An unenriched sample of deoxyribonucleic acid (DNA) was treated in a similar manner to serve as input. NimbleGen ChIP-on-chip protocol (Nimblegen Systems, Inc., Madison, WI, USA) was performed for promoter sequence. The reference sequence human promoter array contained 2.7 kb sequence with 2.2 kb representative of the proximal promoter region and 500 bp of the 5' terminal coding sequence (from National Center for Biotechnology Information Build 36; HG18). Arrays were hybridized and scanned using Agilent Scanner G2505C. Raw data were extracted as. txt files by Agilent Feature Extraction software (version 11.0.1.1) and deposited at the Gene Expression Omnibus (GEO) database with an accession number GSE194415.

#### 2.4. Microarray analysis

Total RNA of KYSE150 cells and CAFs was extracted using mirVana™ RNA isolation kit (Invitrogen, Cat# AM1561). Obtained RNA (0.5 µg) was used for synthesis of Cyanine-3 (Cy3)-labeled cRNA using the One-Color Low RNA Input Linear Amplification PLUS kit (Agilent). Then RNeasy column was used for purification (Qiagen). Dye incorporation and cRNA yield were checked with the NanoDrop ND-2000 spectrophotometer. Microarray was conducted using Agilent SurePrint G3 Human Gene Expression v3 (8 × 60 K). The hybridized arrays were scanned with the Agilent Scanner G2505C microarray scanner, and the data was extracted and normalized using Agilent Feature Extraction software (version 10.7.1.1). Further data analysis was performed using Agilent GeneSpring software (version 13.1). The accession number of microarray data in the GEO database was GSE194414.

#### 2.5. Patient information, tissue specimens and immunohistochemistry (IHC)

Tissue specimens were obtained from patients with ESCC, gastric and colon cancers. Our study was approved by the institutional Review Board of Peking University Cancer Hospital (Beijing, China). For IHC assay, the tissue slides were deparaffinized and antigens were retrieved in high pressure for 15 min with 10 µmol/L Tris-EDTA buffer (pH 9.0). Tissue slides were incubated with the diluted primary antibodies (PAFR antibody was diluted at 1:500, pStat3 Tyr<sup>705</sup> antibody was diluted at 1:100, α-SMA antibody was diluted at 1:3000) at 4 °C overnight. The slides were then washed and incubated with the secondary antibody and stained by DAB substrate, counterstained with hematoxylin, dehydrated and counted. The staining of PAFR and pStat3 Tyr<sup>705</sup> in tissues was scored by the formula: the percentages of positive cells (including: score 0, no positive cells; score 1, <10% positive cells; score 2, 10%–35% positive cells; score 3, 35%–75% positive cells; and score 4, >75% positive cells) × the staining intensity (including: score 1, no staining; score 2, light yellow staining; score 3, yellow brown staining; and score 4, brown staining), scored as 0 to 16. Samples with a staining score ≥8 were considered as high expression and samples with a staining score <8 were defined as low expression.

#### 2.6. Xenograft studies

To evaluate the effect of PAFR/Stat3 axis between KYSE410 or KYSE150 cells and CAFs on tumor growth, the indicated tumor cells, PAFR shRNA, or Stat3 shRNA cells and the indicated CAFs were co-injected subcutaneously into the flank of each animal ( $n = 5/\text{group}$ ). The groups were as follows: tumor cells-shRNA vector alone, tumor cells-shRNA vector + CAFs-shRNA vector, CAFs-PAFR shRNA, or Stat3 shRNA, respectively; tumor cells-PAFR shRNA alone, or +CAFs-shRNA vector, +Stat3 shRNA, respectively; tumor cells-Stat3 shRNA alone, or +CAFs-shRNA vector, +PAFR shRNA, respectively.

For evaluating the effect of PAF/PAFR inhibitor-etizolam and Stat3 inhibitor- S3I-201 on tumor growth, tumor cells and CAFs were co-inoculated subcutaneously into the right flank of each animal ( $n = 5/\text{group}$ ). When tumors reached approximately 80–100 mm<sup>3</sup>, treatments were initiated. The drug therapy was performed with following categories ( $n = 5/\text{group}$ ): etizolam low

or high dose (1 mg/kg/day or 10 mg/kg/day, daily oral gavage) alone, S3I-201 (25 mg/kg, daily oral gavage), low or high dose of etizolam combined with S3I-201. Animals were randomized to receive the above treatments. The inhibitory efficiency of each agent alone or their combination was examined for approximately 26 days. Tumor sizes were calculated by Eq. (1):

$$\text{Tumor size (mm}^3\text{)} = (\text{Length} \times \text{Width}^2) \times 0.5 \quad (1)$$

Animal handling and procedures were ethically approved by the Animal Center, Peking University Cancer Hospital (Beijing, China).

#### 2.7. Statistical analysis

The detailed information about statistic and methods is indicated in figure captions, main text or methods. The measurements of all statistical values were performed using Graphpad Prism 7.0 (GraphPad Software Inc., La Jolla, CA, USA), unless otherwise described in the figure legends or methods. Error bars in the experiments indicate standard deviation (SD) for a minimum of three independent experiments.

Other methods were provided in “Supporting Information” section.

### 3. Results

#### 3.1. Stat3 is activated in CAFs surrounding tumor cells

The activated form of Stat3-pStat3 Tyr<sup>705</sup> is overexpressed in the nuclear of tumor cells and associated with tumor malignant progression. To evaluate whether Stat3 is activated in tumor micro-environment (TME), we used IHC assay to observe the staining intensity of pStat3 Tyr<sup>705</sup> in the nuclei of tumor-associated stroma within clinical epithelial-derived gastrointestinal cancer samples, including ESCC, gastric, colorectal, and rectal cancers. Stromal cells exist in the interstitial spaces of cancer tissues. Tumor-adjacent normal tissues were used for comparison in where invariably low or negative nuclear pStat3 Tyr<sup>705</sup> was staining. However, stromal cells frequently present remarkable nuclear pStat3 Tyr<sup>705</sup> staining in close proximity to tumor cells (Fig. 1A–D).

α-Smooth muscle actin (α-SMA), often as a marker for CAFs, however, is not exist in normal fibroblasts<sup>24,25</sup>. We stained tumor sections for pStat3 Tyr<sup>705</sup> and α-SMA using sequential slides. We found that most of the pStat3 Tyr<sup>705</sup> positive stromal cells coexisted with α-SMA (Fig. 1A–D). Furthermore, strong stromal pStat3 Tyr<sup>705</sup> expression was positively correlated with advanced-stage, higher-grade tumor status and lymph node status of cancer patients (Fig. 1E–H). Interestingly, results of Fig. 1E–H reveal that the expression of stromal pStat3 and proximity tumor pStat3 were tightly associated. Cancer patients were then divided into 4 groups based on stromal/tumor pStat3 expression levels. The stromal pStat3 Tyr<sup>705</sup> (high)/tumor pStat3 Tyr<sup>705</sup> (high) group had the shortest overall survival times, compared with other three groups (Fig. 1E–H).

#### 3.2. Stat3 regulates PAFR expression both in tumor and CAFs

To explore the functional relationship between tumor and CAFs and to investigate whether this connection is under the control of

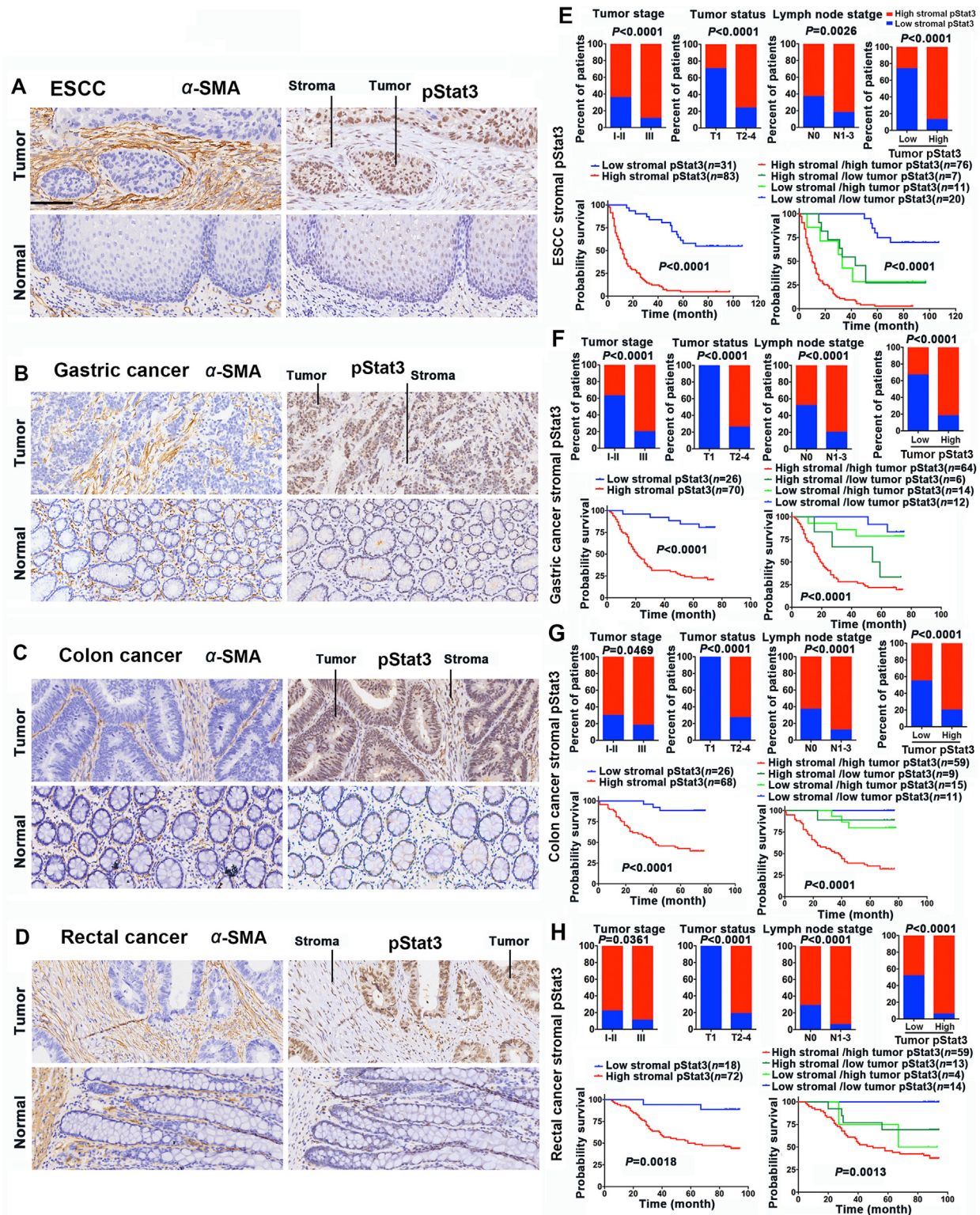


**Figure 1** The expression of pStat3 in tumor cells and CAFs is correlated with the malignancy of gastrointestinal cancers. (A–D) Representative images for immunohistochemical pStat3 (Tyr<sup>705</sup>) and  $\alpha$ -SMA staining in sequential slides of ESCC ( $n = 114$ ) (A), gastric ( $n = 96$ ) (B), colon ( $n = 94$ ) (C), or rectal ( $n = 90$ ) (D) cancers and their neighboring normal tissues. Magnification:  $10\times$  as indicated. (E–H) Percentages of ESCC (E, upper panel), gastric cancer (F, upper panel), colon cancer (G, upper panel), rectal cancer (H, upper panel) patients with high expression of stromal pStat3 and low expression of stromal pStat3 according to different clinical parameters as follows: tumor stage, tumor status, lymph node status and the expression of tumoral pStat3. Two-tailed Pearson  $\chi^2$  test. Kaplan–Meier curves of ESCC (E), gastric cancer (F), colon cancer (G), or rectal cancer (H) patients with low versus high expression of stromal pStat3 or stromal/tumor pStat3 co-expression with overall survival (lower panel). Log-rank test,  $P$  values were indicated.



These results indicate that Stat3 activity regulates PAFR abundance in both tumor cells and CAFs. We also assessed whether inhibition of Stat3 activity suppressed the transcriptional expression of some representative, including *CPT1C*, *IL11*, *HBEGF*, *OSBPL2*, *IL7R*, *ZIC2*, *CAMKK2*, *IL6*, *AXL*, and *RHOA* using real-time PCR, and found that 25  $\mu\text{mol/L}$  S3I-201 effectively inhibited the expression of molecules in KYSE410, or KYSE150 cells and CAFs (Supporting Information Fig. S1A–S1J).

Overexpression of PAFR was significantly correlated with higher clinical stage of ESCC patients<sup>23</sup>. We identified the positive correlation between PAFR and pStat3 Tyr<sup>705</sup> in gastrointestinal cancers and their stroma (Supporting Information Fig. S2A–S2H). The patients with strong coexpression of PAFR and pStat3 Tyr<sup>705</sup> in gastrointestinal cancers, or stroma had shortest overall survival times according to Kaplan–Meier analysis (Supporting Information Fig. S3A–S3D). Interestingly, PAFR or pStat3 Tyr<sup>705</sup> expression in tumors was positively correlated with either pStat3 or PAFR expression in CAFs, respectively (Fig. S2A–S2H). The stromal pStat3/tumor PAFR or tumor pStat3/stromal PAFR group could also be used to effectively predict the survival of patients (Fig. S3A–S3D).

### 3.3. PAFR induces Stat3 activity involving the formation of tyrosine kinase 2 (Tyk2)/Janus kinase 2 (JAK2) heterodimer complex

Our previous study has demonstrated that the level of PAF was higher in ESCC tumors than adjacent normal tissues<sup>23</sup>. In present study, we evaluated the concentration of PAF in KYSE410, KYSE150 cells and CAFs using enzyme linked immunosorbent assay (ELISA), and found that PAF was highly secreted from these cells (Supporting Information Fig. S4). We found that PAF/PAFR axis could stimulate Stat3 in ESCC cells<sup>23</sup>. To deeply clarify how PAF/PAFR axis activated Stat3 signaling, we analyzed the activity changes of JAK2 (the upstream tyrosine kinase of Stat3) and Stat3 in indicated ESCC control cells or ESCC cells treated with 100 nmol/L PAF, or condition medium (CM) from CAFs. JAK2 or Stat3 activity was markedly increased following 100 nmol/L PAF or CAFs CM treatment in indicated ESCC cells (Fig. 3A–C, Supporting Information Fig. S5A and S5B). However, depletion of PAFR or the antagonist of PAF-WEB2086 (50  $\mu\text{mol/L}$ ) effectively blocked PAF and CAFs-stimulated JAK2 or Stat3 activity in ESCC cells (Fig. 3A–C, Fig. S5A and S5B).

PAFR associates with the Tyk2/JAK2 heterodimer complex in a PAF-regulated manner in COS-7 cells<sup>26,27</sup>. Tyk2 activates JAK2 via forming Tyk2/JAK2 protein complex in myeloproliferative neoplasms (MPN)<sup>28</sup>. However, the existence of PAFR/Tyk2/JAK2 protein complex and the role of PAFR on Tyk2-activated JAK2 in solid tumor cells are unclear. We next examined the physical association between PAFR/Tyk2/JAK2 complex, and found that PAFR co-existed in the same protein complex with Tyk2 and JAK2 under the stimulation of 100 nmol/L PAF or CAFs CM (Fig. 3D). Immunoprecipitation assays showed that 50  $\mu\text{mol/L}$  WEB2086 disrupted the formation of PAFR/Tyk2/JAK2 protein complex or JAK2 activation in this complex induced by 100 nmol/L PAF or CAFs CM (Fig. 3D). Results of Fig. 3E revealed that PAFR shRNA blocked the formation of Tyk2/JAK2 complex and the activation of JAK2 in this protein complex. Furthermore, PAFR D289A mutant, which inhibits PAFR to couple to G-proteins, was used to evaluate whether the formation of Tyk2/JAK2 heterodimer

complex is dependent on the PAFR-activated small G-proteins. Our results indicate that PAFR D289A mutant had no effect on the formation of Tyk2/JAK2 heterodimer complex and JAK2 activation (Fig. 3F and G). Additionally, PAF or CAFs CM-activated Stat3 could be inhibited by JAK2 inhibitors—ruxolitinib or fedratinib (Fig. 3H). Taken together, above results demonstrate that PAFR formed complex with Tyk2 and JAK2 to activate JAK2/Stat3 pathway in tumor cells. Furthermore, CM from KYSE410 or KYSE150 cells and 100 nmol/L PAF promoted the assembly of PAFR/Tyk2/JAK2 complex in CAFs (Supporting Information Fig. S6).

### 3.4. Reciprocal regulation of PAFR/Stat3 signaling between tumor and CAFs

To determine whether PAFR in tumor cells affected PAFR/Stat3 axis in CAFs, we compared PAFR and pStat3 abundance in CAFs treated with the CM from PAFR-positive control or PAFR-depleted tumor cells (Fig. 4A). CAFs were treated with the CM from PAFR-depleted ESCC cells as compared with that from PAFR-positive control ESCC cells, and our results found that PAFR-positive KYSE410 or KYSE150 cells could induce the expression of PAFR and the activation of Stat3 in CAFs, whereas PAFR-depleted ESCC cells not (Fig. 4B). We then evaluated whether the upregulation of PAFR from tumor cells to CAFs was Stat3-dependent. The CM from PAFR-positive tumor cells upregulate PAFR expression in Stat3-positive but not in Stat3-knockdown CAFs (Fig. 4B). However, the CM from PAFR-knockdown tumor cells produced no significant effects on PAFR expression in CAFs with or without Stat3 (Fig. 4B). These results suggest that PAFR-positive tumor cells could regulate Stat3-dependent PAFR expression in CAFs.

Reciprocally, KYSE410 or KYSE150 cells growing in CM from PAFR-positive control CAFs showed enhanced PAFR and pStat3 expression compared with tumor cells cultured alone (Fig. 4C and D). However, the CM from PAFR-depleted CAFs could not effectively induce the activation of PAFR and Stat3 in tumor cells, indicating that CAFs harboring high level of PAFR can also regulate PAFR and pStat3 abundance in tumor cells (Fig. 4D). Correspondingly, PAFR-positive CAFs could effectively upregulate the NF- $\kappa$ B activity in ESCC cells, broadening the PAFR-activated signaling pathways under the TME milieu (Fig. 4E).

We further examined whether abundant PAFR expression in tumor cells would contribute to the secretion of Stat3-related cytokines-IL-6 or IL-11 from CAFs (Fig. 4F). Results of Fig. 4G demonstrate that CM from PAFR-positive ESCC cells enhanced the secretion of IL-6 and IL-11 from CAFs, both of which were Stat3-dependent. In addition, Fig. 4H reveals that IL-6, or IL-11 neutralizing antibody (Ab) inhibited the indicated ESCC cells CM-induced PAFR and pStat3 expression in CAFs.

The secretion of IL-6 and IL-11 was upregulated from KYSE410 and KYSE150 cells cultured with the CM from control CAFs, but not with that of PAFR-depleted CAFs (Supporting Information Fig. S7). Moreover, CM from PAFR-positive CAFs treatment effectively promoted the secretion of IL-6 and IL-11 in control ESCC cells, but not in Stat3-depleted ESCC cells (Fig. S7). Furthermore, adding IL-6, or IL-11 Ab to *in vitro* culture of tumor cells reduced CAFs-mediated PAFR and pStat3 abundance in ESCC cells, indicating that cytokines are the major mediator of PAFR/Stat3 signaling (Fig. 4I).

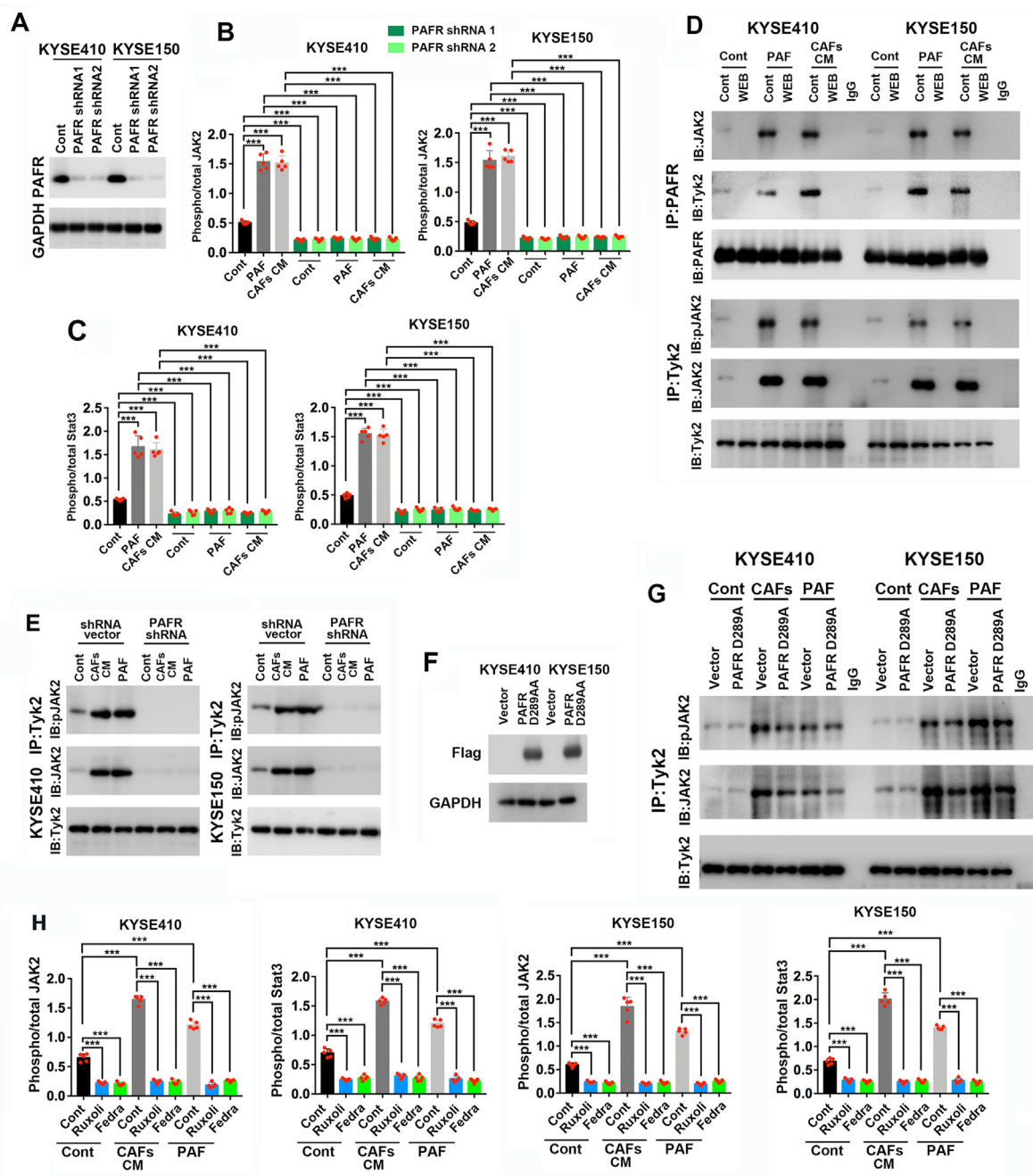


**Figure 3** PAFR induces Stat3 activity involving the formation of Tyk2/JAK2 heterodimer complex. (A) Silencing PAFR in two specific shRNA-transduced stable ESCC cell lines analyzed by immunoblotting (right panel). GAPDH was used as a loading control. (B, C) The indicated ESCC cells were treated with 100 nmol/L PAF, or CM from CAFs. The JAK2 (B) or Stat3 (C) activity was assayed by JAK2 or Stat3 activation quantitative ELISA. Data are shown as mean  $\pm$  SD ( $n = 5$ ,  $***P < 0.001$ , by two-tailed unpaired Student's  $t$ -test). (D) Immunoprecipitation assay revealed that 100 nmol/L PAF or CM from CAFs more effectively increased PAFR interacted with JAK2 and Tyk2 (upper panel) or the activation of JAK2 (Tyr<sup>1007/1008</sup>) in Tyk2/JAK2 complex (lower panel) both in KYSE410 and KYSE150 cells. PAF antagonist WEB2086 (50  $\mu$ mol/L) significantly disrupted the interaction between PAFR and JAK2 or Tyk2, or the activation of JAK2 (Tyr<sup>1007/1008</sup>) in Tyk2/JAK2 complex in KYSE410 or KYSE150 cells alone or treated with 100 nmol/L PAF or CM from CAFs. (E) Transfection of PAFR shRNA into the indicated ESCC cells effectively disrupted the interaction between PAFR and JAK2 or Tyk2, or the activation of JAK2 (Tyr<sup>1007/1008</sup>) in Tyk2/JAK2 complex of ESCC cells treated with 100 nmol/L PAF or CM from CAFs. (F) PAFR D289A plasmid transfected into KYSE410 and KYSE150 cells and immunoblotting was applied for evaluating the transfection efficacy. GAPDH was used as a loading control. (G) Transfection of PAFR D289A plasmid into the indicated ESCC cells did not disrupt the interaction between Tyk2 and JAK2 and block the activation of JAK2 (Tyr<sup>1007/1008</sup>) in Tyk2/JAK2 complex. (H) JAK2 inhibitors (5  $\mu$ mol/L ruxolitinib, 5  $\mu$ mol/L fedratinib) effectively inhibited 100 nmol/L PAF or CM from CAFs-activated JAK2/Stat3 signaling in KYSE410 and KYSE150 cells. Data in bar graph are shown as mean  $\pm$  SD ( $n = 5$ ,  $***P < 0.001$ , by two-tailed unpaired Student's  $t$ -test).

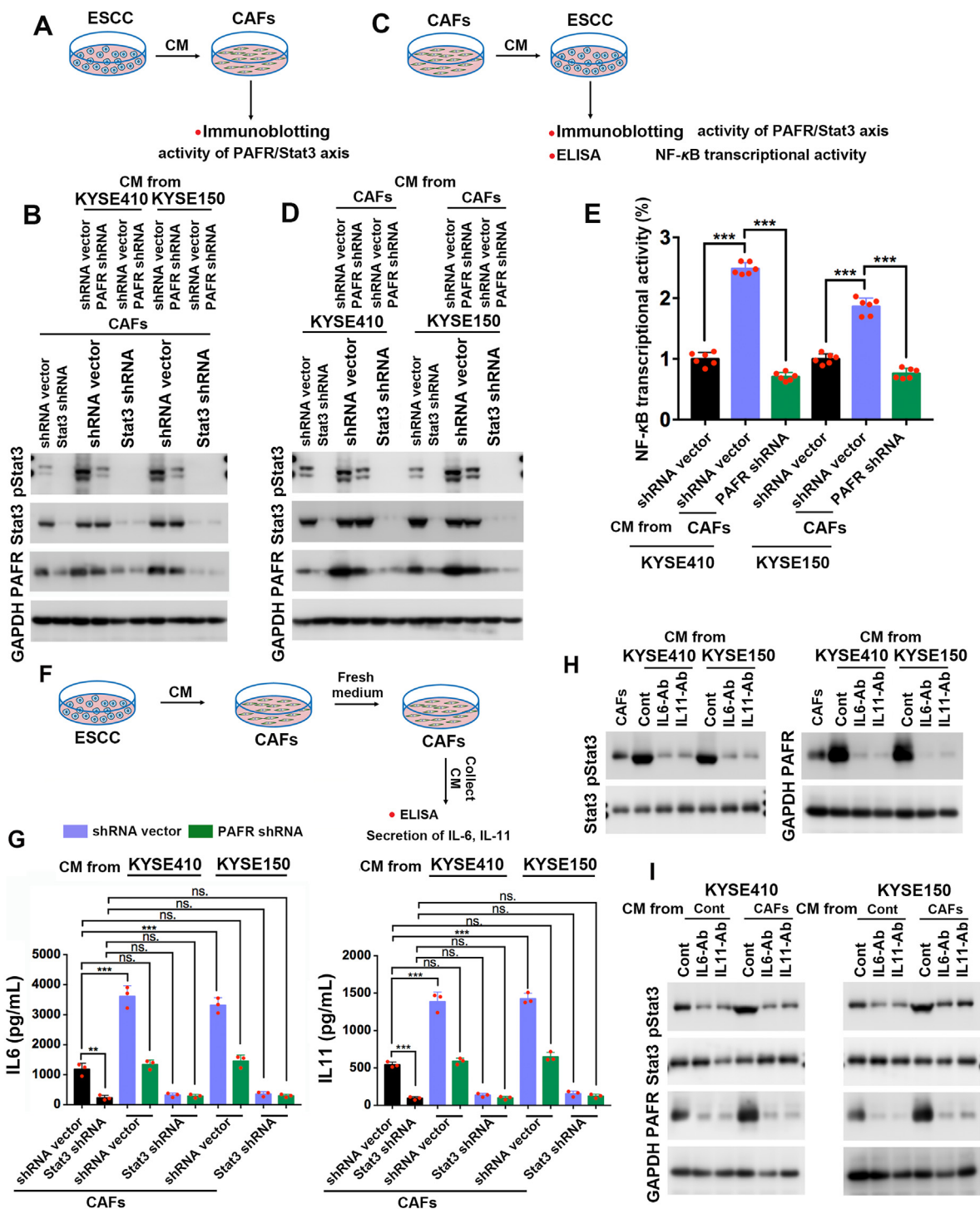


**Figure 4** Reciprocal regulation of PAFR and Stat3 between ESCC and CAFs. (A) Protocol of immunoblotting assay. (B) Immunoblotting showing that the expression of pStat3 Tyr<sup>705</sup>, Stat3, or PAFR in CAFs harbored with shRNA control vector or Stat3 shRNA incubated in the presence or absence of the CM from KYSE410 or KYSE150 cells transfected with shRNA control vector or PAFR shRNA. (C) Protocol of immunoblotting and NF-κB activity assay. (D) Immunoblotting showing that the expression of pStat3 Tyr<sup>705</sup>, Stat3, or PAFR in KYSE410 or KYSE150 cells harbored with shRNA control vector or Stat3 shRNA incubated in the presence or absence of the CM from CAFs transfected with shRNA control vector or PAFR shRNA. (E) NF-κB p65 transcriptional factor activity assay indicating that NF-κB activity in KYSE410, KYSE150 alone or in the presence of the CM from CAFs transfected with shRNA control vector or PAFR shRNA. Data are shown as mean ± SD ( $n = 6$ ,  $***P < 0.001$ , by two-tailed unpaired Student's  $t$ -test). (F) Protocol of ELISA. (G) ELISA showing that the secreted-IL-6 or IL-11 in the supernatant of CAFs harbored with shRNA control vector or Stat3 shRNA incubated with/without the CM from KYSE410 and KYSE150 cells transfected with shRNA control vector or PAFR shRNA. Data are shown as mean ± SD ( $n = 3$ ,  $**P < 0.01$ ,  $***P < 0.001$ , ns. represents no significant difference, by two-tailed unpaired Student's  $t$ -test). (H) Immunoblotting showing that the expression of pStat3 Tyr<sup>705</sup>, Stat3, or PAFR in CAFs treated with CM from the indicated ESCC cells alone or in the presence of IL-6, or IL-11 neutralizing antibody (10 μg/mL). (I) Immunoblotting showing that the expression of pStat3 Tyr<sup>705</sup>, Stat3, or PAFR in KYSE410, KYSE150, alone or in the presence of CAFs CM co-treated with control solvent, IL-6, or IL-11 neutralizing antibody (10 μg/mL).

### 3.5. PAFR/Stat3 signaling in tumor cells and CAFs coordinately promotes tumor progression

We further evaluated the contribution of PAFR/Stat3 crosstalk between ESCC and CAFs to the malignant proliferation of ESCC cells

using 3-(4,5-dimethylthiazol-2-yl)-5-(3-carboxymethoxyphenyl)-2-(4-sulfophenyl)-2H-tetrazolium, inner salt (MTS) assay *in vitro*. As shown in Fig. 5A and B, ESCC cells cultured with the CM from CAFs displayed stronger growth ability compared with ESCC cells alone. However, ESCC cells cultured with the CM from Stat3 or

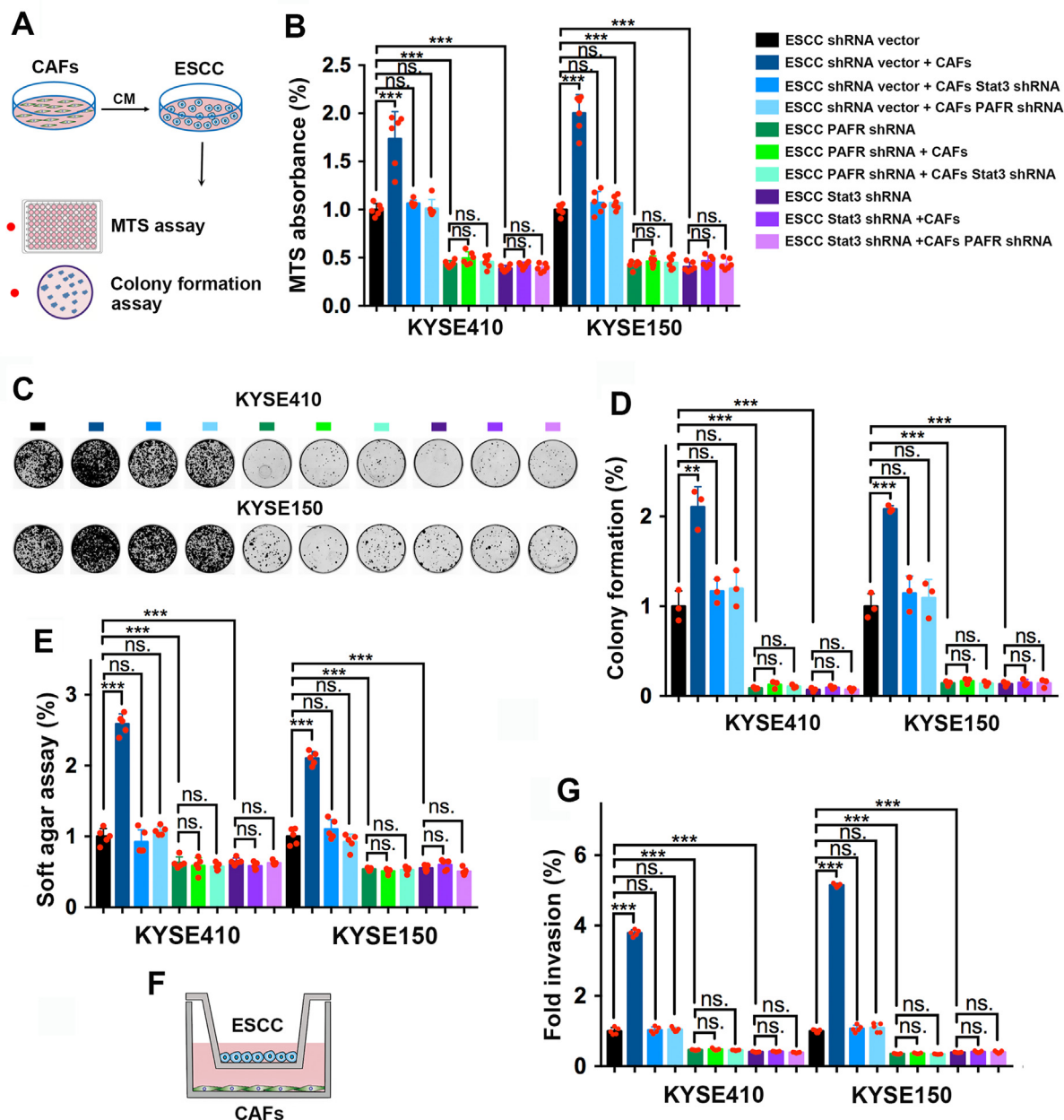


**Figure 5** Crosstalk of PAFR/Stat3 signaling between ESCC cells and CAFs promotes tumor malignancy *in vitro*. (A) Protocol of cellular assays. (B) MTS assay indicating that KYSE410, KYSE150 cells or their Stat3, or PAFR shRNA counterpart cells were incubated with the CM from control CAFs, Stat3, or PAFR shRNA CAFs, respectively for 4 days. Data are shown as mean  $\pm$  SD ( $n = 6$ ,  $***P < 0.001$ , ns. represents no significant difference, by two-tailed unpaired Student's *t*-test). (C) Colony formation assay indicating that KYSE410, KYSE150, or their Stat3, or PAFR shRNA counterpart cells were incubated with the CM from control CAFs, Stat3, or PAFR shRNA CAFs, respectively for 10 days. (D) Quantitation of colony formation in (C). Data in bar graph are shown as mean  $\pm$  SD ( $n = 3$ ,  $**P < 0.01$ ,  $***P < 0.001$ , ns. represents no significant difference, by two-tailed unpaired Student's *t*-test). (E) Soft agar assay. KYSE410, KYSE150 cells or their Stat3, or PAFR shRNA counterpart cells were incubated with the CM from control CAFs, Stat3, or PAFR shRNA CAFs, respectively, for 8 days. Data in bar graph are shown as mean  $\pm$  SD ( $n = 5$ ,  $***P < 0.001$ , ns. represents no significant difference, by two-tailed unpaired Student's *t*-test). (F) Schematic of invasion assay. (G) Transwell assay indicating that KYSE410, KYSE150, or their Stat3, or PAFR shRNA counterpart cells (upper chamber) were plated alone or cocultured with control CAFs, CAFs Stat3, or PAFR shRNA (lower chamber) in Transwell apparatus with 8  $\mu$ m pore size for 16 h. Data are shown as mean  $\pm$  SD ( $n = 5$ ,  $***P < 0.001$ , ns. represents no significant difference, by two-tailed unpaired Student's *t*-test).

PAFR-depleted CAFs could not enhance the growth ability compared with ESCC cells alone. Furthermore, PAFR or Stat3 depletion substantially suppressed proliferation of ESCC cells. The CM from CAFs, Stat3, or PAFR-depleted CAFs could not enhance the proliferation of PAFR, or Stat3-depleted ESCC cells. Similar results were also obtained in anchorage-dependent or independent colony formation assay (Fig. 5C–E).

Boyden chambers were applied to examine the invasion of ESCC cells by plating them on matrigel-coated inserts with CAFs in the lower wells (Fig. 5F). As shown in Fig. 5G, control CAFs effectively enhanced the invasiveness of the indicated ESCC cells compared with ESCC cells alone, whereas not the Stat3, or PAFR-depleted CAFs. PAFR or Stat3 depletion effectively inhibited the invasion of ESCC cells compared with control ESCC cells

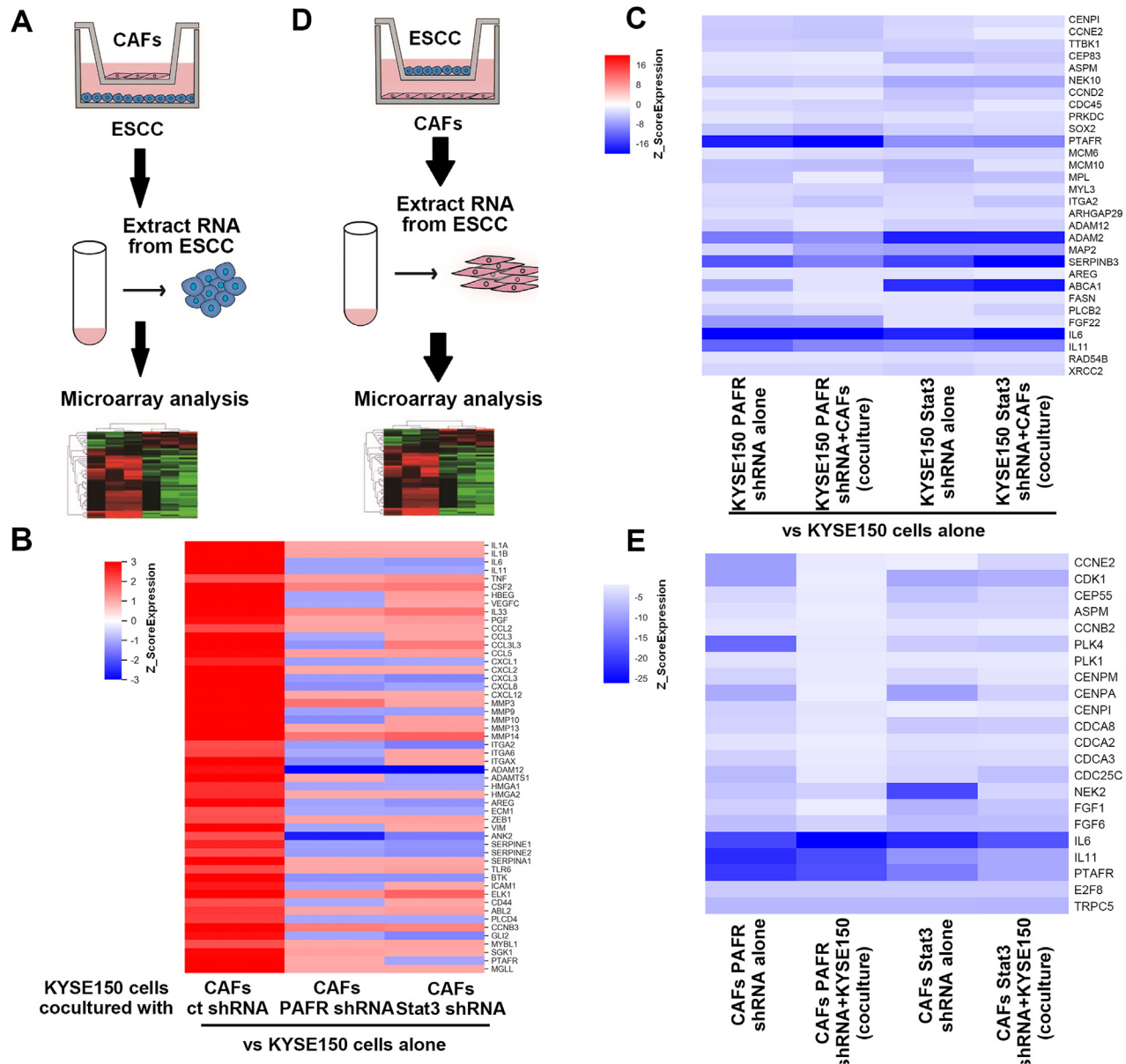


**Figure 6** PAFR/Stat3 axis drives mutual transcriptional programming of ESCC cells and CAFs. (A) Schematic showing that control, Stat3 or PAFR shRNA KYSE150 cells (lower chamber) co-cultured with control, Stat3 or PAFR shRNA CAFs (upper chamber) in Transwell apparatus with 0.4  $\mu\text{m}$  pore size for 24 h. RNA was extracted from the indicated KYSE150 cells and subjected to microarray assay. (B) Heatmap representing upregulated expression of genes (fold change  $\geq 2$ ) of KYSE150 cells cocultured with indicated CAFs vs. KYSE150 cells alone. The expression of these upregulated genes was not significantly activated (fold change  $< 2$ ) in KYSE150 cells co-cultured with Stat3 or PAFR shRNA CAFs. (C) Heatmap representing downregulated expression of genes (fold change  $\geq 2$ ) of PAFR or Stat3 shRNA KYSE150 cells vs. control shRNA KYSE150 cells. The expression of these downregulated genes was not significantly activated (fold change  $< 2$ ) in PAFR or Stat3 shRNA KYSE150 cells co-cultured with CAFs. (D) Schematic showing that control, Stat3 or PAFR shRNA CAFs (lower chamber) co-cultured with indicated KYSE150 cells (upper chamber) in Transwell apparatus with 0.4  $\mu\text{m}$  pore size for 24 h. (E) Heatmap representing downregulated expression of genes (fold change  $\geq 2$ ) of PAFR or Stat3 shRNA CAFs vs. control shRNA CAFs. The expression of these downregulated genes was not significantly activated (fold change  $< 2$ ) in PAFR or Stat3 shRNA CAFs co-cultured with KYSE150 cells.

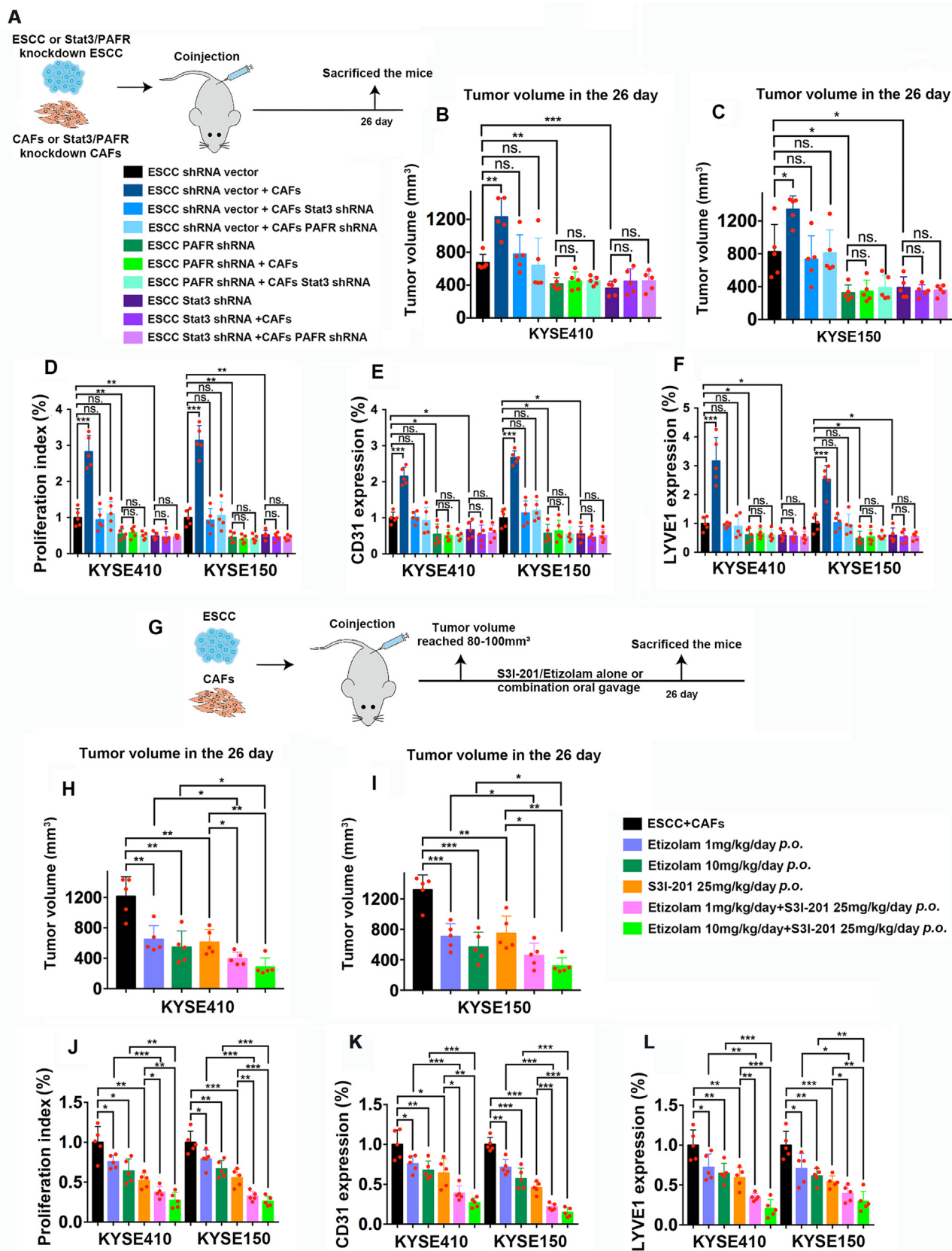


**Figure 7** Crosstalk of PAFR/Stat3 signaling between ESCC cells and CAFs promotes tumor malignancy *in vivo*. (A) ESCC and CAFs co-injection xenograft model. (B, C) Tumor volume of mice bearing KYSE410 (B), KYSE150 (C) tumors or their Stat3, or PAFR shRNA counterpart tumors alone or co-injection with CAFs, CAFs Stat3, or PAFR shRNA cells in 26 days. Data are shown as mean  $\pm$  SD ( $n = 5$ ,  $*P < 0.05$ ,

(Fig. 5G). Furthermore, control CAFs, Stat3, or PAFR-depleted CAFs co-cultured with ESCC cells could not enhance the invasion of PAFR, or Stat3-depleted ESCC cells (Fig. 5G).

### 3.6. Stromal PAFR/Stat3 axis drives a transcriptional program in tumor cells that promotes malignant phenotypes

Co-culture system (Transwell apparatus with 0.4  $\mu\text{m}$  pore size) was used to evaluate the effect of CAFs on the expression of tumor-promoting-related genes in ESCC cells, the upper chamber was plated with CAFs, and the lower chamber was cultured with KYSE150 cells (Fig. 6A). The RNA of KYSE150 cells was extracted and hybridized it to gene expression arrays. The expression of genes altered by  $\geq 2$ -fold was considered significant, and the enriched upregulation gene set was mainly related to cytokine signaling, chemokine signaling, invasion and metastasis signaling, proliferation signaling, and inflammation signaling (Fig. 6B and Supporting Information Table S4). However, PAFR or Stat3 knockdown CAFs could not significantly upregulate the control CAFs-stimulated gene expression in KYSE150 cells, compared to KYSE150 cells alone (Fig. 6B and Supporting Information Tables S5 and S6).

Depletion of PAFR or Stat3 in KYSE150 cells was observed to effectively inhibit the expression of genes involved in cell cycle signaling, proliferation signaling, invasion and metastasis signaling, metabolism, cytokine signaling, and DNA repair signaling, compared with KYSE150 cells alone (Fig. 6C, and Supporting Information Tables S7 and S8). Importantly, CAFs could not significantly upregulate the expression of above PAFR or Stat3 depletion-inhibited genes in ESCC cells (Fig. 6C, Supporting Information Tables S9 and S10). Thus, in fibroblasts, PAFR/Stat3 axis stimulates a transcriptional program likely to promote tumor progression *via* stimulating the expression of intratumoral PAFR/Stat3 pathway-controlled tumor malignant genes.

### 3.7. Stromal PAFR/Stat3 signaling drives a transcriptional program in CAFs that supports malignant cells

We further investigated how co-culture with ESCC cells affects PAFR/Stat3 axis-dependent gene expression in stromal fibroblasts. We collected the CAFs cells from the lower chamber of Transwell apparatus with 0.4  $\mu\text{m}$  pore size, extracted RNA, and hybridized it to gene expression arrays. The upper chamber of Transwell apparatus was plated with KYSE150 cells (Fig. 6D). Co-culture with ESCC cells upregulated a series cluster of genes in CAFs, involved in cytokine signaling, chemokine signaling, invasion and metastasis signaling, metabolism and growth (Supporting Information Table S11).

Co-downregulated genes in PAFR or Stat3-depleted CAFs were included cell cycle signaling, proliferation signaling, and cytokine signaling, compared with CAFs alone (Fig. 6E, and

Supporting Information Tables S12 and S13). Importantly, KYSE150 cells co-culture could not upregulate the expression of above downregulated genes in PAFR or Stat3-depleted CAFs, respectively compared with these two CAFs alone (Fig. 6E, Supporting Information Tables S14 and S15). Thus, stromal fibroblasts respond to ESCC cells in a manner that supports tumor malignancy, whereas depletion of PAFR/Stat3 axis in CAFs does not support for ESCC malignant progression.

### 3.8. PAFR/Stat3 crosstalk between tumor and CAFs contributes to the malignant progression of tumor in vivo

To further determine whether PAFR/Stat3 crosstalk between ESCC and CAFs contributes to the malignant progression of ESCC *in vivo*, we co-implanted KYSE410 or KYSE150 cells subcutaneously into mice with PAFR/Stat3-positive control or PAFR/Stat3-knockdown CAFs (Fig. 7A). CAFs effectively induced tumor growth of ESCC compared with ESCC tumor alone (Fig. 7B and C, Supporting Information Fig. S8A and S8B). However, without PAFR/Stat3 axis in CAFs, ESCC tumor failed to grow compared with ESCC cells co-injected with control CAFs. Furthermore, PAFR-depleted ESCC tumors grew slower than control ESCC tumors, and CAFs could not effectively facilitate the growth of PAFR-depleted ESCC tumors. Similarly, Stat3-depleted ESCC tumors grew slower than control ESCC tumors even co-injected with CAFs. The malignant progression of ESCC tumors was also reflected by the proliferative (Ki67 index), angiogenic (platelet endothelial cell adhesion molecule 1; PECAM1/CD31 expression), or lymphangiogenic (lymphatic vessel endothelial hyaluronin acid receptor 1 (LYVE1) expression) marker (Fig. 7D–F). Our data indicate that the mutual regulation of PAFR and Stat3 between tumor cells and CAFs that synergistically induce tumor malignancy.

### 3.9. PAFR and Stat3 inhibitors synergize in suppressing tumor growth in vivo

It was crucial to investigate whether the synergistic inhibition of PAFR/Stat3 axis between tumor and CAFs could produce tumor-suppressing effect. ESCC tumor cells were co-injected with CAFs subcutaneously into the right flank of nude mice. When tumors reached approximately 80–100  $\text{mm}^3$ , mice were treated with Stat3 inhibitor—S3I-201 (25 mg/kg, daily oral gavage), PAFR/PAFR inhibitor—etizolam (1 or 10 mg/kg/day, daily oral gavage), and S3I-201 plus etizolam (two combination groups: 25 mg/kg/day S3I-201 plus 1 mg/kg/day etizolam, and 25 mg/kg/day S3I-201 plus 10 mg/kg/day etizolam, respectively) (Fig. 7G). Our results demonstrate that the cotreatment of S3I-201 and etizolam caused a considerably decreased tumor volume in comparison with both low and high doses of each agent alone (Fig. 7H and I, Supporting Information Fig. S8C and S8D). Furthermore,

**\*\*P < 0.01, \*\*\*P < 0.001, ns.** represents no significant difference, by two-tailed unpaired Student's *t*-test). (D–F) Ki-67 (D), CD31 (E), LYVE1 (F) index was used to quantitatively analyze the proliferative ability, angiogenesis, lymph vessel formation of xenografted tumors. Data are shown as mean  $\pm$  SD ( $n = 5$ , \* $P < 0.05$ , \*\* $P < 0.01$ , \*\*\* $P < 0.001$ , ns. represents no significant difference, by two-tailed unpaired Student's *t*-test). (G) ESCC and CAFs co-injection xenograft model with different drugs treatment. (H, I) Tumor volume of mice bearing KYSE410 (H) or KYSE150 (I) co-injection with CAFs treated with lower (1 mg/kg/day, daily oral gavage) or higher (10 mg/kg/day, daily oral gavage) dose of etizolam (PAFR inhibitor), Stat3 inhibitor-S3I-201 (25 mg/kg/day, daily oral gavage) alone or their combination in 26 days. Data are shown as mean  $\pm$  SD ( $n = 5$ , \* $P < 0.05$ , \*\* $P < 0.01$ , \*\*\* $P < 0.001$ , by two-tailed unpaired Student's *t*-test). (J–L) The expression of Ki-67 (J), CD31 (K), LYVE1 (L) was applied to analyze the proliferative ability, angiogenesis, lymph vessel formation of xenografted tumors using ELISA. Data are shown as mean  $\pm$  SD ( $n = 5$ , \* $P < 0.05$ , \*\* $P < 0.01$ , \*\*\* $P < 0.001$ , by two-tailed unpaired Student's *t*-test).

combination of S3I-201 and etizolam effectively inhibited the expression of Ki67, CD31 and LYVE1 in ESCC tumors (Fig. 7J–L).

We assessed the serum level of IL-6 and IL-11 in ESCC/CAFs coinjection mouse model, and found that co-injection CAFs with KYSE410 or KYSE150 cells could effectively upregulate the serum concentration of IL-6 and IL-11, compared with KYSE410 or KYSE150 cells alone (Supporting Information Fig. S9A and S9B). Importantly, Inhibition of PAFR/Stat3 axis by the combination of etizolam and S3I-201 effectively decreased the serum level of IL-6 and IL-11 in ESCC cells/CAFs coinjection mouse model (Supporting Information Fig. S9C and S9D).

#### 4. Discussion

The mechanism of symbiotic relationship between tumor and stroma are complicated. In the present study, we demonstrated that Stat3 played a key role in facilitating the stroma from a tumor-repressive environment to a supportive one by transcriptional reprogramming. The activated stromal Stat3 was tightly correlated with poor outcome in human gastrointestinal cancers, including ESCC, gastric, colorectal, and rectal cancers. Using high-throughput screening we found that several promoters were co-empowered by Stat3 both in tumor cells and CAFs. These molecules were involved in cell growth and invasion, metabolism, transcriptional activity, ion channel, protein kinase, stemness, cytokine signaling or stress-induced proteins, suggesting that cancer cells and stromal cells may possibly produce the similar biological effect to maintain the symbiotic status between tumor and stroma under the microenvironmental stress. Among these detected promoters, we focused on the *PAFR* gene promoter, a critical molecule was hyperactivated in these gastrointestinal cancers according to our previous study<sup>23</sup>, and showed that the significantly clinical correlation between pStat3 and PAFR in tumor cells and stromal CAFs. Taken together, our study highlights that PAFR/Stat3 signaling may possibly be the driving force to facilitate the communication between tumor cells and stroma. Further mechanical investigations on the other Stat3-regulated promoters are critical for our understanding of the interaction between tumor and stroma.

Stat3 supports the malignant of tumor cells in a multitude of ways, including cell cycle, DNA repair, metabolism, and proliferation<sup>29–32</sup>, especially interacting with GPCRs and various tyrosine kinases to induce tumor progression<sup>33–36</sup>. Our previous work has entirely focused on tumor autonomous PAFR-related signaling pathways<sup>23</sup>. In the present study, we reveal that the stromal PAFR/Stat3 axis facilitated pathways that are also benefit to the malignancy, including angiogenesis, ECM organization, adhesion, and migration. Combination with the results that PAFR/Stat3 axis-regulated transcriptional program in tumor cells, our data suggest that stromal Stat3 facilitates a reciprocal symbiosis between stroma and cancer cells, and the coordination of Stat3 between tumor cells and stroma fuels the malignant state. Mechanistically, the crosstalk of PAFR/Stat3 signaling between tumor cells and CAFs was also observed and can be, at least partly, mediated by Stat3-dependent IL-6 and IL-11 secretion. On account of directly upregulating PAFR expression, the activated Stat3 was modulated by these two defined cytokines, exerted an effect on tumor cells and CAFs to respond to PAF. Taken together, these findings indicate that activated-PAFR/Stat3 axis between tumor and CAFs can act in positive feedback loops to induce a

reciprocal communication between tumor and stroma. This symbiotic relationship between CAFs and cancer cells instructs a tumor/microenvironment ecosystem that facilitates malignant progression of cancer.

Our previous study reported that the important inflammation-associated transcriptional factor-NF- $\kappa$ B can also actively form feed-forward activation loop with PAFR in ESCC cells<sup>23</sup>. Here, we found that the expression status of PAFR in CAFs could also determine the activity of NF- $\kappa$ B in ESCC cells, indicating that stromal PAFR signaling can also regulate the PAFR-controlled pathways in ESCC cells. Maintenance of NF- $\kappa$ B activity in tumors requires persistent Stat3 activation, which prolongs NF- $\kappa$ B nuclear retention and interfere with NF- $\kappa$ B nuclear export<sup>37,38</sup>. Correspondingly, CAFs can upregulate various NF- $\kappa$ B-related molecules in tumor cells, whereas not the PAFR and Stat3-depleted CAFs. Therefore, our study highlights that PAFR/Stat3 axis in both tumor cells and CAFs can master two inflammatory factors and may synergistically mediate cancer-related inflammation.

It appears that GPCRs can utilize tyrosine kinases to exert their cellular effects<sup>39,40</sup>. Therefore, we further attempted to demonstrate the tyrosine kinases—JAKs-related mechanism of PAFR-activated Stat3. Our results show that PAFR, independent of its coupled small G proteins, formed protein complex with Tyk2/JAK2 under the stimulation of PAF or CAFs, indicating that the physiological importance of PAFR on the activation of JAK2/Stat3 signaling under the microenvironment stress. Formation of Tyk2/JAK2 heterodimerization can induce the resistance of MPN cells to JAK2 inhibitors<sup>28</sup>. However, the biological significance of Tyk2/JAK2 in solid tumors is still unclear. Present study confirms that the existence of Tyk2/JAK2 heterodimerization in solid tumor and further shows that PAFR is the critical initiator for facilitating the formation of this heterodimerization. Taken together, our results demonstrate that PAFR/Tyk2/JAK2 heterodimerization can promote the activation of JAK2/Stat3 signaling and provide a novel mechanism of oncogenic driver-mediated assembly of Tyk2/JAK2 protein complex under microenvironmental stress.

Furthermore, different from other oncogenic receptors, GPCRs can seemingly not be self-activated. Its functional activation requires the presence of ligand<sup>41,42</sup>. Meanwhile, the expression of PAFR is the rate-limiting factor in the activation of PAF/PAFR cascade by virtue of the kinetics of PAF and PAFR binding features an extremely slow off-rate. Correspondingly, regulation of PAFR levels in both tumor and CAFs cells can also regulate the Stat3 activity in other cells, further indicating that cancer cells and their microenvironments can effectively rewire and reprogram the signaling pathways to coordinate to induce tumor progression. According to these believes, the synergistic interaction between etizolam, a specific PAF/PAFR antagonist with anti-anxiety activity and classical Stat3 inhibitor-S3I-201, were observed on tumor growth *in vivo* with tumor cocultured with CAFs xenograft model. We used lower doses of etizolam and S3I-201 to demonstrate synergy for particular co-culture of tumor and its microenvironment model in xenograft model, and observed a dramatic grow-inhibitory effect on tumors when lower doses of etizolam and S3I-201 were combined compared with each agent alone even at their higher dose combination. Correspondingly, these results strengthen the possibility of adding agents that are comparatively nontoxic to the specific pathway inhibitors to the treatment of solid tumors. The hyperexpression of PAFR both in ESCC and stroma has significant diagnostic implication. Evaluation of PAFR expression in both ESCC cells and stroma may assist to guide

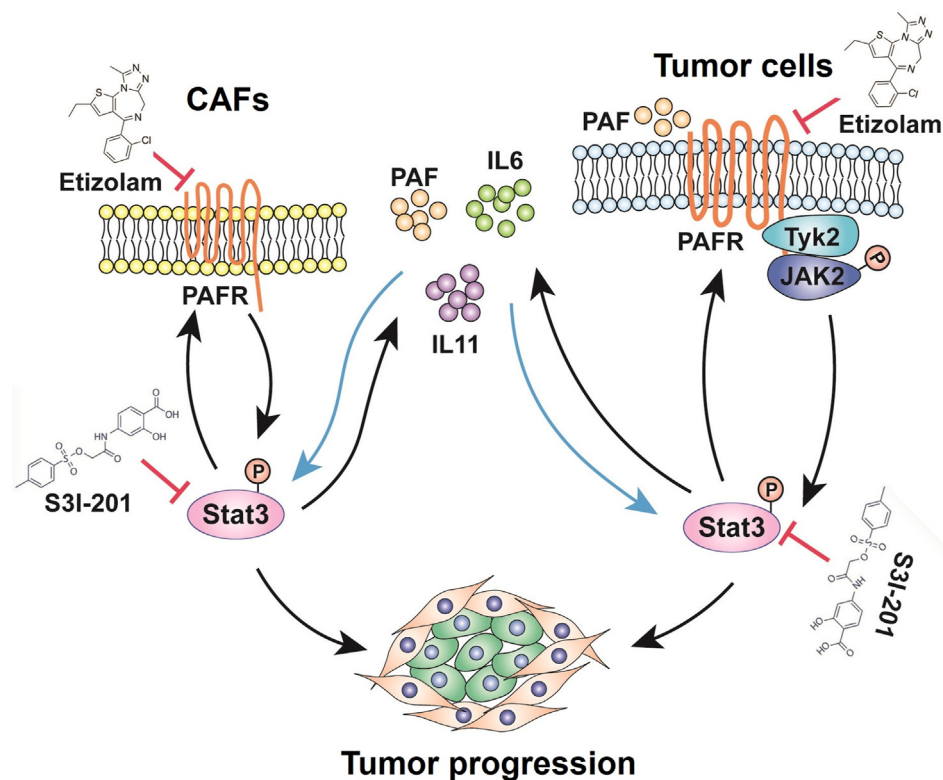


**Figure 8** Proposed model of coinhibition of PAFR and Stat3 axis suppresses ESCC malignancy. PAFR/Stat3 axis mediates the crosstalk of signaling pathways between CAFs and tumor cells, and drives similar downstream signaling networks in transcription. IL-6 and IL-11 play key roles in PAFR/Stat3 axis-mediated crosstalk between tumors and CAFs. Coinhibition of PAFR and Stat3 activities effectively blocked the progression of tumor.

treatment choices in different stages of ESCC, where currently there are no reliable biomarkers for judging the malignant extent<sup>43</sup>. Our findings indicate that PAFR activated both in stroma and ESCC cells provide opportunity for exploring co-owned biomarkers in tumor and TME that not relying solely on the targeting of mutated intratumoral molecules.

## 5. Conclusions

Our findings suggest that PAFR-mediated tumor microenvironment modulation and tumor malignant progression is at least in part mediated by Stat3. Many tumor-promoting cytokines not only activate Stat3 but also interacts with PAF/PAFR axis, and PAF/PAFR/Stat3 in turn promotes the production of these cytokines, thus linking Stat3 signaling directly with the PAF/PAFR axis in the tumor microenvironment milieu. Their co-regulation in both tumor cells and stromal cells may have profound biological and therapeutic implications for cancer and other inflammatory diseases (Fig. 8).

## Acknowledgments

This study was supported by National Natural Science Foundation of China (Nos. 81988101, 81830086, and 81972243, China), CAMS Innovation Fund for Medical Sciences (No. 2019-I2M-5-081, China), Guangdong Basic and Applied Basic Research Foundation (No. 2019B030302012, China).

## Author contributions

Qimin Zhan and Jie Chen designed the experiments and wrote the paper. Di Zhao, Jing Zhang, Lingyuan Zhang, Qingnan Wu, Yan Wang, Weimin Zhang, and Yuanfan Xiao performed the experiments and analyzed the data.

## Conflicts of interest

The authors declare no conflicts of interest.

## Appendix A. Supporting information

Supplementary data to this article can be found online at <https://doi.org/10.1016/j.apsb.2022.08.014>.

## References

1. Kalluri R. The biology and function of fibroblasts in cancer. *Nat Rev Cancer* 2016;**16**:582–98.
2. Kobayashi H, Enomoto A, Woods SL, Burt AD, Takahashi M, Worthley DL. Cancer-associated fibroblasts in gastrointestinal cancer. *Nat Rev Gastroenterol Hepatol* 2019;**16**:282–95.
3. Kwa MQ, Herum KM, Brakebusch C. Cancer-associated fibroblasts: how do they contribute to metastasis?. *Clin Exp Metastasis* 2019;**36**: 71–86.
4. Chen X, Song E. Turning foes to friends: targeting cancer-associated fibroblasts. *Nat Rev Drug Discov* 2019;**18**:99–115.

5. Kashima H, Noma K, Ohara T, Kato T, Katsura Y, Komoto S, et al. Cancer-associated fibroblasts (CAFs) promote the lymph node metastasis of esophageal squamous cell carcinoma. *Int J Cancer* 2019; **144**:828–40.
6. Zhao G, Li H, Guo Q, Zhou A, Wang X, Li P, et al. Exosomal Sonic Hedgehog derived from cancer-associated fibroblasts promotes proliferation and migration of esophageal squamous cell carcinoma. *Cancer Med* 2020; **9**:2500–13.
7. Qiao Y, Zhang C, Li A, Wang D, Luo Z, Ping Y, et al. IL6 derived from cancer-associated fibroblasts promotes chemoresistance via CXCR7 in esophageal squamous cell carcinoma. *Oncogene* 2018; **37**: 873–83.
8. Zhang H, Xie C, Yue J, Jiang Z, Zhou R, Xie R, et al. Cancer-associated fibroblasts mediated chemoresistance by a FOXO1/TGFBeta1 signaling loop in esophageal squamous cell carcinoma. *Mol Carcinog* 2017; **56**:1150–63.
9. Du X, Xu Q, Pan D, Xu D, Niu B, Hong W, et al. HIC-5 in cancer-associated fibroblasts contributes to esophageal squamous cell carcinoma progression. *Cell Death Dis* 2019; **10**:873.
10. Yeo SY, Ha SY, Lee KW, Cui Y, Yang Z, Xuan Y, et al. Twist1 is highly expressed in cancer-associated fibroblasts of esophageal squamous cell carcinoma with a prognostic significance. *Oncotarget* 2017; **8**:65265–80.
11. Chen J, Wang Y, Zhang W, Zhao D, Zhang L, Zhang J, et al. NOX5 mediates the crosstalk between tumor cells and cancer-associated fibroblasts via regulating cytokine network. *Clin Transl Med* 2021; **11**: e472.
12. Huynh J, Chand A, Gough D, Ernst M. Therapeutically exploiting STAT3 activity in cancer-using tissue repair as a road map. *Nat Rev Cancer* 2019; **19**:82–96.
13. Yu H, Lee H, Herrmann A, Buettner R, Jove R. Revisiting STAT3 signalling in cancer: new and unexpected biological functions. *Nat Rev Cancer* 2014; **14**:736–46.
14. Darnell Jr JE. Transcription factors as targets for cancer therapy. *Nat Rev Cancer* 2002; **2**:740–9.
15. Lavecchia A, Di Giovanni C, Novellino E. STAT-3 inhibitors: state of the art and new horizons for cancer treatment. *Curr Med Chem* 2011; **18**:2359–75.
16. Haura EB, Turkson J, Jove R. Mechanisms of disease: insights into the emerging role of signal transducers and activators of transcription in cancer. *Nat Clin Pract Oncol* 2005; **2**:315–24.
17. Groner B, Lucks P, Borghouts C. The function of Stat3 in tumor cells and their microenvironment. *Semin Cell Dev Biol* 2008; **19**:341–50.
18. Johnson DE, O'Keefe RA, Grandis JR. Targeting the IL-6/JAK/STAT3 signalling axis in cancer. *Nat Rev Clin Oncol* 2018; **15**:234–48.
19. Crusz SM, Balkwill FR. Inflammation and cancer: advances and new agents. *Nat Rev Clin Oncol* 2015; **12**:584–96.
20. Xing F, Saidou J, Watabe K. Cancer associated fibroblasts (CAFs) in tumor microenvironment. *Front Biosci* 2010; **15**:166–79.
21. Albregues J, Bertero T, Grasset E, Bonan S, Maiel M, Bourget I, et al. Epigenetic switch drives the conversion of fibroblasts into proinvasive cancer-associated fibroblasts. *Nat Commun* 2015; **6**:10204.
22. Huynh J, Etemadi N, Hollande F, Ernst M, Buchert M. The JAK/STAT3 axis: a comprehensive drug target for solid malignancies. *Semin Cancer Biol* 2017; **45**:13–22.
23. Chen J, Lan T, Zhang W, Dong L, Kang N, Zhang S, et al. Platelet-activating factor receptor-mediated PI3K/AKT activation contributes to the malignant development of esophageal squamous cell carcinoma. *Oncogene* 2015; **34**:5114–27.
24. Kalluri R, Zeisberg M. Fibroblasts in cancer. *Nat Rev Cancer* 2006; **6**: 392–401.
25. Quante M, Tu SP, Tomita H, Gonda T, Wang SS, Takashi S, et al. Bone marrow-derived myofibroblasts contribute to the mesenchymal stem cell niche and promote tumor growth. *Cancer Cell* 2011; **19**:257–72.
26. Lukashova V, Asselin C, Krolewski JJ, Rola-Pleszczynski M, Stanková J. G-protein-independent activation of Tyk2 by the platelet-activating factor receptor. *J Biol Chem* 2001; **276**:24113–21.
27. Lukashova V, Chen Z, Duhé RJ, Rola-Pleszczynski M, Stanková J. Janus kinase 2 activation by the platelet-activating factor receptor (PAFR): roles of Tyk2 and PAFR C terminus. *J Immunol* 2003; **171**:3794–800.
28. Koppikar P, Bhagwat N, Kilpivaara O, Manshoury T, Adli M, Hricik T, et al. Heterodimeric JAK–STAT activation as a mechanism of persistence to JAK2 inhibitor therapy. *Nature* 2012; **489**:155–9.
29. Lankadasari MB, Aparna JS, Mohammed S, James S, Aoki K, Binu VS, et al. Targeting S1PR1/STAT3 loop abrogates desmoplasia and chemosensitizes pancreatic cancer to gemcitabine. *Theranostics* 2018; **8**:3824–40.
30. Cao D, Qi Z, Pang Y, Li H, Xie H, Wu J, et al. Retinoic acid-related orphan receptor C regulates proliferation, glycolysis, and chemoresistance via the PD-L1/TGFB6/STAT3 signaling axis in bladder cancer. *Cancer Res* 2019; **79**:2604–18.
31. Lee M, Hirpara JL, Eu JQ, Sethi G, Wang L, Goh BC, et al. Targeting STAT3 and oxidative phosphorylation in oncogene-addicted tumors. *Redox Biol* 2019; **25**:101073.
32. Chang JC. Cancer stem cells: role in tumor growth, recurrence, metastasis, and treatment resistance. *Medicine (Baltimore)* 2016; **95**: S20–25.
33. Ho MK, Su Y, Yeung WW, Wong YH. Regulation of transcription factors by heterotrimeric G proteins. *Curr Mol Pharmacol* 2009; **2**:19–31.
34. Burger M, Hartmann T, Burger JA, Schraufstatter I. KSHV-GPCR and CXCR2 transforming capacity and angiogenic responses are mediated through a JAK2/STAT3-dependent pathway. *Oncogene* 2005; **24**: 2067–75.
35. Zhou M, Mok MT, Sun H, Chan AW, Huang Y, Cheng AS, et al. The anti-diabetic drug exenatide, a glucagon-like peptide-1 receptor agonist, contracts hepatocarcinogenesis through cAMP–PKA–EGFR–STAT3 axis. *Oncogene* 2017; **36**:4135–49.
36. Lee HJ, Zhuang G, Cao Y, Du P, Kim HJ, Settleman J. Drug resistance via feedback activation of Stat3 in oncogene-addicted cancer cells. *Cancer Cell* 2014; **26**:207–21.
37. Lee H, Herrmann A, Deng JH, Kujawski M, Niu G, Li Z, et al. Persistently activated Stat3 maintains constitutive NF- $\kappa$ B activity in tumors. *Cancer Cell* 2009; **15**:283–93.
38. Grivennikov SI, Karin M. Dangerous liaisons: STAT3 and NF- $\kappa$ B collaboration and crosstalk in cancer. *Cytokine Growth Factor Rev* 2010; **21**:11–9.
39. Vázquez-Juárez E, Ramos-Mandujano G, Hernández-Benítez R, Pasantes-Morales H. On the role of G-protein coupled receptors in cell volume regulation. *Cell Physiol Biochem* 2008; **21**:1–14.
40. Piiper A, Zeuzem S. Receptor tyrosine kinases are signaling intermediates of G protein-coupled receptors. *Curr Pharmaceut Des* 2004; **10**:3539–45.
41. Deupi X, Kobilka B. Activation of G protein-coupled receptors. *Adv Protein Chem* 2007; **74**:137–66.
42. Smith NJ, Milligan G. Allosteric at G protein-coupled receptor homo- and heteromers: uncharted pharmacological landscapes. *Pharmacol Rev* 2010; **62**:701–25.
43. Lin DC, Wang MR, Koeffler HP. Genomic and epigenomic aberrations in esophageal squamous cell carcinoma and implications for patients. *Gastroenterology* 2018; **154**:374–89.